IEEE Open Journal of the
Industrial Electronics Society

Received 20 July 2023; revised 10 October 2023; accepted 20 October 2023. Date of publication 31 October 2023; date of current version 10 November 2023. The review of this paper was arranged by Associate Editor Gerhard Hancke.

Digital Object Identifier 10.1109/OJIES.2023.3329021

An Energy-Saving LoRa Linear Network System With Adaptive Transmission Parameter

HAO WANG [1], SHANSHAN LV [1], YANG HAN [1], XIHAI ZHANG [1,2] (Member, IEEE), YU ZHANG [1], WENBIN DONG [1], JIANXIN LIAO [1,3], AND HONGWEI LUAN [1]

[1]School of Electrical and Information, Northeast Agricultural University, Harbin 150030, China
[2]National Key Laboratory of Smart Farm Technology and System, Northeast Agricultural University, Harbin 150030, China
[3]State Grid Zoucheng Power Supply Company, Zoucheng 273500, China

CORRESPONDING AUTHORS: XIHAI ZHANG; YU ZHANG (e-mail: xhzhang@neau.edu.cn; zhangyu1900@neau.edu.cn).

This work was supported by the Heilongjiang Province University Discipline Collaborative Innovation Achievement Project under Grant LJGXCG2023-100.

ABSTRACT LoRaWAN is widely used in information monitoring under star topology. However, for linear topology applications, the LoRaWAN protocol requires the introduction of a large number of gateways, which will lead to information asymmetry, energy waste, and low network utilization. An energy-saving LoRa linear network system with adaptive transmission parameter is proposed. LoRa multihop technology is used for communication between nodes in the system, and narrowband Internet of Things module is used to the communicate with cloud platform. The adaptive transmission parameter mechanism is adopted in the system, which improves the adaptability of the linear network to changes in link channel conditions and reduces unnecessary energy consumption. At the same time, the flexibility and robustness of self-organizing networks are enhanced. In addition, optimized duty cycle strategies are employed to further reduce the operating power consumption. After LoRaSim simulation experiments, the results show that in the changing radio channel environment, the adaptive transmission parameter mechanism could achieve a dynamic balance between data extraction rate and energy consumption. After field tests, the results show that the system not only operates stably, but also could reduce the operating energy consumption of the LoRa linear network. The system proposed in this article is suitable for linear topological structure scenes such as river hydrological monitoring, oil pipeline monitoring, and long-distance railway monitoring.

INDEX TERMS Linear topology, LoRa, multihop, narrowband Internet of Things (NB-IoT), wireless sensor network (WSN).

I. INTRODUCTION

The Internet of Things (IoT) is a huge network formed by combining various information sensing devices with the internet [1]. In the past few years, the IoT industry has shown a vigorous development trend and has been widely used in home, transportation, medical care, logistics, and other fields [2], [3], [4]. Wireless sensor networks (WSNs) play an important role in the application of IoT. Linear sensor network (LSN) is a form of WSN, in which sensor nodes are distributed linearly or nonlinearly [5]. This kind of monitoring network is mainly aimed at linear topology monitoring scenarios, such as highway monitoring, long-distance pipeline monitoring for transporting oil, natural gas and water resources, and river environment monitoring. These scenes often require a longer transmission distance and lower energy consumption. Traditional short-range wireless communication technologies such as Bluetooth, Wi-Fi, and ZigBee cannot meet the needs well. Low-power wide-area network (LPWAN) can provide the longest coverage with minimal power consumption [6], and its appearance is expected to solve this problem perfectly.

LoRa is one of the LPWAN communication technologies. LoRa technology's network layer protocol is mainly LoRaWAN, which defines LoRa's system architecture [7]. Since LoRaWAN was founded, it has received extensive attention from academia and industry. El Chall et al. [8] studied the network performance and coverage of the LoRaWAN protocol in three different environments in Lebanon, which confirmed the reliability of LoRaWAN in IoT applications such as intelligent cities and intelligent agriculture. Muzammir et al. [9] studied LoRaWAN's communication performance from packet loss rate, data rate, and communication range, and concluded that its signal strength is suitable for indoor use. Davcev et al. [10] proposed an energy-efficient and highly scalable IoT agricultural system model based on LoRaWAN, and further described the preliminary results of the model applied to vineyards. Yang and Liang [11] proposed a new packet transmission model based on LoRaWAN and applied it in the real elderly care scene. Thus, LoRaWAN's architecture makes it simple to deploy and easy to maintain in star topology scenarios such as smart cities and smart agriculture [12]. However, this transmission method is more suitable for star-network, and there may be data loss and communication errors in other topologies, such as grid structure or linear topology. In addition, through single-hop information exchange, a longer transmission distance means a higher spreading factor (SF) [13], which has a dual impact on the network capacity. It reduces the transmission rate, increases the air broadcast time, and nodes at the edge of the network may lose a large number of data packets due to collisions [14]. Therefore, low power consumption and multihop transmission may be a feasible solution.

At present, the research on LoRa multihop is divided into multihop communication between gateways and multihop communication between nodes. Between gateways, Dwijaksara et al. [15] proposed a multihop G2G communication protocol for LoRa networks, including the routing protocol which is based on the ad hoc on-demand distance vector routing and the MAC protocol for G2G packet transmission, and achieved reasonably good network performance. Farooq et al. [16] proposed a multihop communication protocol for LoRa with software-defined networking extension, which offered maximum coverage at a relatively very high data rate and lower energy consumption. However, when the number of gateways is increased, it often leads to more complex networks, higher collision rate, and internetwork interference. In addition, it will also cause information asymmetry, energy waste, and low network utilization. This strategy is not suitable for linear topology networks. Between nodes, Abrardo et al. [17] presented a LoRa-based multihop linear architecture, which is to be used to monitor the formation of Black Powder in gas pipelines. Abrardo and Pozzebon [18] also presented an LSN topology based on multihop LoRa chain-type communications, which is to be used in the pervasive monitoring system for underground environments. The above-mentioned two multihop networks used a fixed maximum spreading factor (SF=12). Although it achieved the maximum transmission range, it caused energy waste. In the synchronous LoRa mesh network proposed by Ebi et al. [19], a fixed medium spreading factor (SF=9) was chosen. Although it improved the reliability of data packet transmission, when the LoRa radio channel environment changed, the fixed communication parameters were inflexible, which may cause unnecessary energy waste and data packet loss.

Based on the abovementioned, this article proposed an energy-saving LoRa linear system with adaptive transmission parameter (ATP). The proposed system included several system nodes and a cloud server. System nodes consist of LoRa terminals and narrowband IoT (NB-IoT) modules. The function of LoRa terminal is to implement self-organizing network in the system. The NB-IoT module is an internet connector, which is the information link between LoRa terminal and server. During the operation of the system, each system node could read the sensor data and realize data aggregation through LoRa multihop mode. The aggregated data are uploaded to the cloud server by the sink node (gateway) through NB-IoT technology for users to analyze and view. For this linear network system, this article proposed a novel LoRa multihop communication protocol, which is more flexible and has lower power consumption. Through the ATP mechanism and the optimized duty cycling policy, the protocol improved the adaptability of linear networks to changes in channel conditions, at the same time, reduced the power consumption of the system. In addition, the protocol avoided the occurrence of network collapse due to the single point of fault of the gateway, and enabled the system to have flexible self-organizing network ability and positioning ability for fault nodes, which improves the robustness and fault tolerance of the system. After testing, the system can not only operate stably, but also obtain better communication performance without adding additional gateways. This system can meet the basic needs of hydrological monitoring along the river, oil pipeline monitoring, and long-distance railway monitoring.

The rest of this article is organized as follows. In Section II, system architecture and design are proposed. System hardware design is introduced in Section III. The results are analyzed and discussed in Section IV. Finally, Section V concludes this article.

II. SYSTEM ARCHITECTURE AND DESIGN

In this section, ATP mechanism is first introduced, then self-organizing linear network based on ATP is analyzed. Finally, optimized duty cycle strategy and media access control protocol dedicated to reducing power consumption are introduced.

A. ATP MECHANISM

The ATP mechanism is divided into the internode mechanism and the sink node mechanism. In LoRa multihop, the communication between nodes adopts the topology of point-to-point LoRa network. The modulation parameters of all nodes, including SF, bandwidth, and code rate, are the same, but the transmission power is flexible and adjustable. The goal of the ATP mechanism between nodes is to improve the probability of data transmission to the next node. When the transmission from the sending node to the next node fails to arrive or the data is wrong, the mechanism retransmits the data and increases the transmission power (TP), thereby increasing the link budget. The ATP mechanism between nodes is shown in Algorithm 1.

Algorithm 1: ATP Mechanism (Internode).

Input: $TP \in [2\ \text{dBm}, 17\ \text{dBm}]$
Output: TP
$ATP\_Tx\_LIMIT \leftarrow 5$
$ATP\_Tx\_CNT \leftarrow 0$
if uplink transmission **then**
  $ATP\_Tx\_CNT \leftarrow ATP\_Tx\_CNT + 1$
if $ATP\_Tx\_CNT > ATP\_Tx\_LIMIT$ **then**
  $TP \leftarrow TP + 3$
if uplink transmission **then**
$ATP\_Tx\_CNT \leftarrow 0$

Algorithm 2: ATP Mechanism (Sink Node).

Input: $SF \in [7, 12]$, $TP \in [2\ \text{dBm}, 17\ \text{dBm}]$
Output: SF & TP
$SNR_{req} \leftarrow$demodulation floor (current data rate)
$SNR_{avg} \leftarrow \frac{1}{N}\sum_{i=1}^{N} SNR_i$
$SNR_{MAD} \leftarrow \frac{1}{N}\sum_{i=1}^{N} |SNR_i - SNR_{avg}|$
$SNR_{margin} \leftarrow SNR_{avg} - SNR_{MAD} - SNR_{req}$
$Nstep \leftarrow \text{int}\,(SNR_{margin}/3)$
while $Nstep > 0$ & $SF > SF_{min}$ **do**
  $SF \leftarrow SF - 1$
  $Nstep \leftarrow Nstep - 1$
end while
while $Nstep > 0$ & $TP > TP_{min}$ **do**
  $TP \leftarrow TP - 3$
  $Nstep \leftarrow Nstep - 1$
end while
while $Nstep < 0$ & $SF < SF_{max}$ **do**
  $SF \leftarrow SF + 3$
  $Nstep \leftarrow Nstep + 1$
end while

The information transmission process is initiated by the first terminal on the line, and passed to the second terminal through the LoRa technology in accordance with the Modbus protocol. After receiving the data, the second terminal performs a CRC check to ensure the integrity of the data, and then according to the check correctly generates the corresponding status code. If the verification is correct, the terminal first responds with a data packet containing the correct status code to the previous terminal, and then integrates the received data with its own data and transmits it to the next terminal node; if the verification code is wrong, this terminal will return an error status code to the previous terminal, and then it will enter the dormant state. The previous terminal makes a decision based on the received status code. If the status code is correct, it means that the data are received successfully and the terminal enters the dormant state. If the status code is wrong, it means that the data verification failed, the previous terminal will retransmit the data and add 1 to the number of retransmissions. If the sending node does not receive the returned data packet within 10 times of time on air (ToA), the sending node will also retransmit the data and add 1 to the retransmission data. The formula of ToA is shown in the following equation:

$$ToA = \frac{2^{SF}}{BW} N_{symbol} \tag{1}$$

where N_{symbol} is the number of symbols, and BW is the bandwidth.

In LoRa multihop, the goal of the ATP mechanism of the sink node (gateway node) is to achieve a dynamic balance between communication quality and network energy consumption in a changing wireless channel environment. It dynamically senses the channel condition changes of the entire linear network, and determines the appropriate link budget according to the average signal-noise ratio (SNR) and mean absolute deviation (MAD) of all nodes. Then, it independently and quickly adjusts the current transmission parameters and deploys them in all nodes. Different from the star topology network in LoRaWAN, LoRa multihop pays more attention to the overall connectivity of the link, and needs to consider the part of the link with the worst communication quality. Therefore, in order to increase the link budget, when estimating the link budget, the average SNR minus MAD is used as the calculation basis. The ATP mechanism of the sink node is shown in Algorithm 2.

Notably, in the ATP mechanism of the sink node (gateway node), SF could be increased or decreased, and TP could be decreased. However, TP will not be increased since it is done by the mechanism of the nodes.

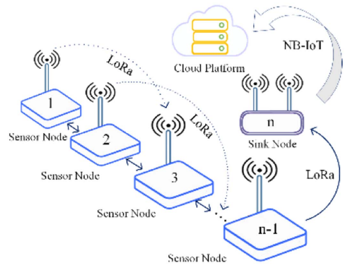

FIGURE 1. System architecture.

B. SELF-ORGANIZING LINEAR NETWORK

The structure of network system with linear topology is shown in Fig. 1, which is mainly composed of a plurality of LoRa sensor node, a gateway node, and a cloud platform. In the process of system operation, a plurality of sensor nodes is arranged on a straight line in sequence, gateway node is positioned at the end of the straight line, sensor information is initiated by the first sensor node on the straight line and transmitted to the second and third sensor nodes through LoRa protocol, according to the above-mentioned steps, information is sequentially transmitted backward and accumulated continuously. The last sensor node that received the information pass the information to gateway node, which gathered the information and uploaded it to the cloud through NB-IoT technology.

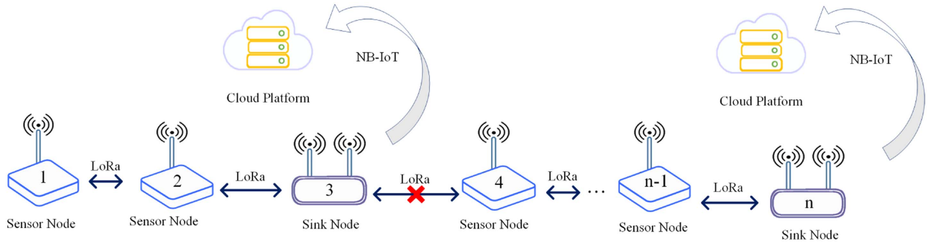

FIGURE 2. New system architecture.

If the transmission power of the node reaches the maximum value, but the returned status code is not received or the returned status code is wrong. The system will mark the next node as "terminal disconnection," skip this node and directly transfer data to the subsequent nodes of this node, which is represented by the dotted line in Fig. 1. If the node still does not receive the response from the subsequent nodes, the node becomes the sink node of the linear network and uploads the system data to the cloud server through the NB-IoT module. If a node does not receive the data sent by the previous node within three wake-up attempts, the node becomes a new starting node to form a new linear network, as shown in Fig. 2. Compared with the LoRa mesh networking system proposed by Cano et al. [20], this method avoids link transmission failure of linear network caused by gateway node failure, ensures the stability of the system and can well locate the faulty node.

C. OPTIMIZED DUTY CYCLE STRATEGY

Low power consumption design is the key to ensure long-term stable operation of the system [21]. In addition to the normal energy consumption of sending and receiving data, data packet collision and overhearing will also cause energy loss for nodes in WSNs [22]. When a node receives multiple data packets at the same time, packet collisions will occur, which will lead to data failure, triggering retransmission mechanism and increasing energy consumption. Overhearing refers to a node receiving data packets destined for other nodes, which is not only useless, but also causes energy waste. According to the above-mentioned facts, in order to reduce power consumption, the system optimizes the duty cycle strategy by adopting asynchronous MAC protocol, reasonably adjusting the low power consumption mode of SX1278 and STM32, and program control sensor power supply ON and OFF.

The SX1278 transceiver used in the system has various modes of operation such as transmission, reception, sleep, standby, and CAD. Generally speaking, most of the power consumption comes from information transmission, reception, and CAD mode. On the contrary, the power consumption in sleep mode is much lower. Therefore, fast sleep after information transmission and reception is an important measure to reduce power consumption. STM32F103ZET6 also has a variety of operating modes. Low power consumption modes include standby mode, stop mode, and sleep mode. According to the function of the node, this design reasonably matches the working modes of the two chips to achieve the purpose of reducing the power consumption of the node. The specific configuration method will be given in Section II-D.

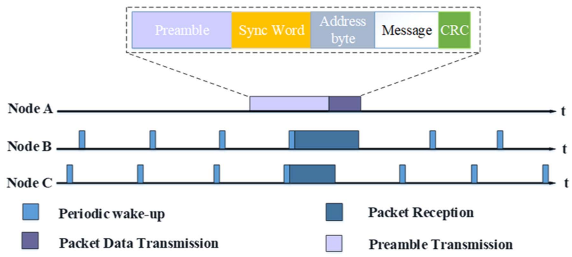

FIGURE 3. Schematic diagram of channel activity detection.

The problem of data packet collision and node overhearing in this system is solved by duty cycle strategy. The communication mode of node information passing back in turn ensures that only one node sends data at a time, so there is no packet conflict. Node information is sent to sleep immediately without idle time, thus reducing energy consumption and avoiding overhearing. From this, it can be seen that using duty cycle strategy in the network can minimize energy waste caused by packet collision and overhearing behavior. In addition, at the very low sampling frequency of the monitoring system, long-term power supply to sensors and modules is also an excessive consumption. The system further saves energy by supplying power to the sensor only during wake-up.

D. MEDIA ACCESS CONTROL PROTOCOL

Media access control is one of the key design issues, because it is directly related to the operation of the transceiver, which is the most resource-consuming component in the node except the processor and sensor unit [22]. Existing MAC protocols are divided into synchronous and asynchronous types. Asynchronous MAC protocol does not need time synchronization, each node can schedule sleep according to its own arrangement, and asynchronous working mode can reduce collisions caused by traffic bursts in the network. In this system, asynchronous MAC protocol initiated by the sender was adopted, and low power consumption interception was realized through CAD algorithm without synchronous process. The following is a detailed description with specific examples.

As shown in Fig. 3, the same channel includes three nodes A, B, and C, node A is the sending node, node B is the

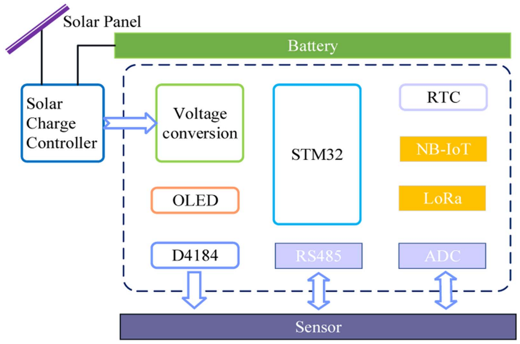

FIGURE 4. System hardware block diagram.

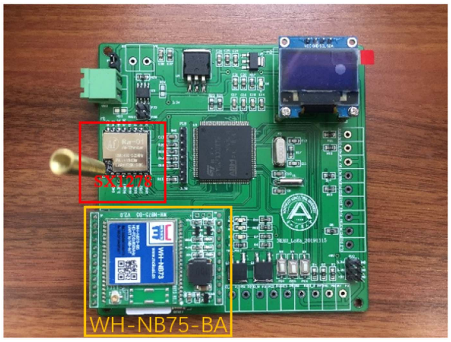

FIGURE 5. Picture of system node.

receiving node, and node C is the normal node. At first, the SX1278 of node A enters sleep mode, and the STM32 of node A enters standby mode. At the same time, nodes B and C operate with duty cycle strategy, the SX1278 and STM32 of the node enter sleep mode, and then enter the CAD mode to see if data needs to be transmitted, and if not immediately enter sleep state. At a certain moment, node A starts to transmit data to node B, and the transmitted data packet includes five parts: preamble, sync word, address byte, message, and CRC. The preamble is used to wake up the receiver. Nodes B and C will wake up after listening to the preamble signal. First, data stream synchronization is completed according to sync word, and then packet filtering is completed through address byte. If the data packet is sent to node B, only node B will successfully match, keep working state and continue to receive data message and complete CRC check. Node C will fail to match, and the chip will switch to sleep mode immediately to prolong the service life of the battery. The CAD algorithm completes low power listening through the above-mentioned process. In order to prevent wireless nodes from missing valid data, it is necessary to ensure that the preamble transmission time length will be slightly longer than the node sleep time.

III. SYSTEM HARDWARE DESIGN

The hardware consists of a plurality of system nodes. Each node is mainly composed of five parts, namely a power supply module, a main control module, a sensor module, a low power consumption circuit, and a communication module, and its structure is shown in Fig. 4. The system nodes use the LoRa module SX1278 for intersystem communication, and use the NB-IoT module WH-NB75-BA to communicate with the cloud platform [23]. The picture of system node is shown in Fig. 5.

The hardware mainly realizes the functions of sensor data acquisition, low power consumption wake-up, and wireless sensor networking. Next, each module component is introduced. In terms of the sensor part, the board card reserved 8 channels of Analog-to-digital converter and 1 channel of RS485 bus interface to be compatible with various industrial sensors, making the system more versatile. The RS485 bus used SP3485 chip, which is a 3.3 V low power half-duplex transceiver, allowing up to 32 transceivers to be connected on the same serial bus, increasing the sensor access capability of the system.

In terms of the power supply part, a 7.4 V 20 000 mAh lithium battery was used, and a 10 W solar panel and a solar charging controller were matched to match the characteristic of flexible change of system node positions. When there is sufficient sunshine, part of the electric energy generated by the solar panel supplies power to the hardware system, and the other part charges the lithium battery. When the sunlight is weak or there is no sunlight, the lithium battery provides energy for the system.

The low power consumption part included sensor power supply ON–OFF circuit and real-time clock (RTC) standby wake-up circuit. The sensor power supply ON–OFF circuit used a high-power MOS tube model D4184 to control. When the information of the sensor needed to be read, power was supplied to the sensor, otherwise no power was supplied. The RTC standby wake-up circuit included a 32.768 KHz crystal oscillator circuit and a button cell circuit. RTC circuit can enable the master to enter a low power consumption mode and reduce power consumption [24].

Wireless sensor networking includes LoRa and NB-IoT. LoRa communication part adopted Ra-01 module, the core of which is SX1278 chip produced by Semtech company. SX1278 has strong flexibility and it can change physical layer parameters such as bandwidth, SF, and coding rate. SX1278 has a high sensitivity of over −148 dBm and a power amplifier of +20 dBm, which provide a longer transmission distance and higher reliability for the monitoring system. To eliminate the differences between networks, NB-IoT module was added. NB-IoT is a new technology in the field of IoT, which supports the cellular data connection of low-power devices in WAN. Operators can directly improve the existing cellular base stations, thus reducing deployment costs and realizing smooth upgrade. WH-NB75-BA used in this design supports CoAP protocol and UDP/TCP protocol. Through configuration, two-way transparent transmission from serial port to network can be realized, simplifying the construction of cloud platform for monitoring system.

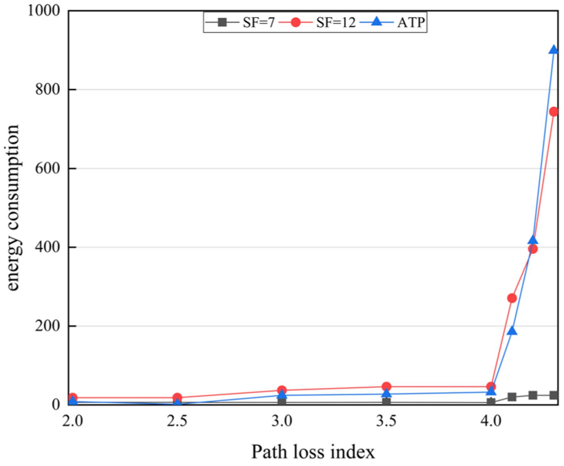

FIGURE 6. Data extraction rate.

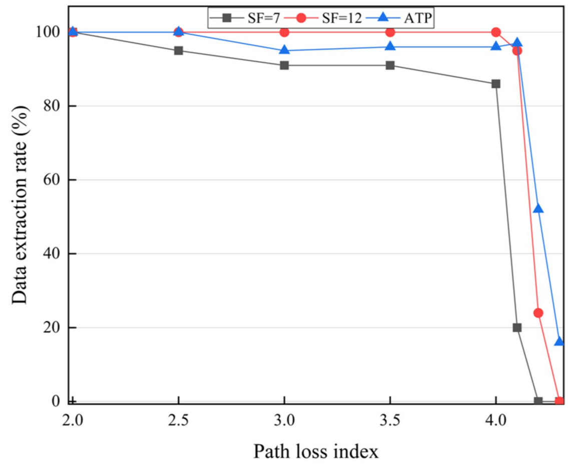

FIGURE 7. Network power consumption.

IV. RESULTS AND DISCUSSION

In order to evaluate the performance of the linear network system, a series of simulation experiments and field tests were carried out, including LoRaSim simulation, point-to-point transmission test, self-organizing network test, working current test, and system comprehensive test.

A. LORASIM SIMULATION

In this article, the LoRaSim simulation tool [25] was used to compare and analyze the three transmission parameter selection strategies. In the simulation scene, a linear network consisting of 20 nodes was set up, and the distance between nodes was 600 m. The path loss index was usually introduced to measure the fading of radio channels. By setting eight groups of different path loss indexes, the channel condition changes of node communication were simulated. The first selection strategy was the fixed selection of the minimum value of SF (SF=7), which was proposed by Mai and Kim [27] in a minimized latency multihop LoRa network protocol. The second selection strategy was the fixed selection of the maximum value of SF (SF=12), which was proposed by the work in [17] and [18]. In a multihop LoRa LSN for the monitoring of underground environments. The third strategy was the transmission parameter adaptive mechanism proposed in this article. In the simulation experiment, in order to analyze the network performance of different selection strategies in different radio channel environments, the data extraction rate and network energy consumption were used as the basis for comparison. The simulation results are shown in Figs. 6 and 7.

From the experimental results, it is clear that when the path loss index increases and the radio channel environment becomes worse, the transmission parameter adaptive mechanism achieves high data extraction rate and low power consumption. Especially, when the path loss index is greater than 4, the radio channel environment becomes more severe. The transmission parameter adaptation mechanism adopts the maximum value of the TP and the maximum value of the SF. Although the energy consumption increases, it achieves higher communication quality.

FIGURE 8. Test environment and physical photos.

B. FIELD TEST

1) POINT-TO-POINT TRANSMISSION TEST

The communication distance of nodes is closely related to the channel conditions of the link, which is an important factor that affects the received signal strength indication (RSSI) and network coverage. In order to evaluate the communication performance of LoRa nodes in this system, the communication distance between LoRa nodes was tested.

As shown in Fig. 8, Northeast Agricultural University was selected as the test environment, and the outdoor temperature

TABLE 1. RSSI SNR Lost Change With Distance

Position	Distance (km)	RSSI (dBm)	SNR (dB)	Lost (%)
Position 1	0	–12	25	0
Position 2	0.23	–84	24	0
Position 3	0.46	–89	23	0
Position 4	0.69	–101	–26	0
Position 5	0.92	–102	–14	7.69
Position 6	1.15	–112	–21	0
Position 7	1.38	–114	–40	38
Position 8	1.61	–	–	100
Position 9	1.84	–	–	100
Yellow star	1.868	–109	–7	0

was −25 °C. In the test process, two sensor nodes were selected as test objects, and one of them was set as a fixed node and the other was set as a mobile node. The fixed node was marked Position 1. The mobile node changed from Positions 2 to 9 in sequence. Their positions are shown in Fig. 8. The horizontal distance between adjacent nodes is 0.23 km. The physical layer parameters of the two nodes are consistent, the SF is 7, the bandwidth is 125 KHz, and the antenna gain is 2.5 dBi. The fixed node sent data every 20 s, and the mobile node calculated RSSI and SNR values after receiving the data, and obtained the time interval between the two data packets. These data can be used to calculate the packet loss rate. The test results are shown in Table 1.

Table 1 shows the relationship between node distance and RSSI, SNR, and packet loss rate. According to the table, with the increase of distance, the RSSI and SNR values show a downward trend and the packet loss rate increases continuously. The maximum RSSI value is −12 dBm and the minimum RSSI value is −114 dBm at Position 7. For Positions 1–3, the SNR is positive, and the signal energy is much higher than the noise. It is worth noting that the SNR value of Position 4 (−26 dB) is lower than that of Position 5 (−14 dB). The main reason is that Position 4 is behind the teaching building, and the signal attenuation causes the noise to increase. When the distance increases to 1.61 km, the packet loss rate is 100%, but stable data RSSI value of −109 and SNR value of 7 are received in the yellow pentagram area beside Position 9, and there is no packet loss. The effective transmission distance of LoRa in this test is only 1.15 km, mainly because obstacles and radio interference in complex campus environment affect the transmission distance between two points [26]. However, the linear connection between the transmitting node and the yellow pentagram area can avoid the main buildings, so stable data transmission can be obtained. The linear distance between the fixed node and the yellow pentagram area is 1.868 km, which is much larger than 1.15 km, further illustrating the influence of environmental factors on LoRa.

More importantly, in the LoRa node, when the SF is 7 and BW is 125 KHz, the minimum SNR value that could be demodulated is −7.5 dB, and the minimum RSSI value that could be demodulated is −126.5 dBm. However, in Table 1, the SNR values of positions 4–7 are all less than −7.5 dB, and the node could still realize data transmission. Because the RSSI values at the above-mentioned positions are all less than −126.5 dBm, the connectivity of the LoRa link is determined by the relatively poorer of the RSSI and SNR. In an obscured communication environment, the SF of the node was set to 7, and then point-to-point transmission test was performed. The test results show that when the SNR value reaches −73 dB and the RSSI value is −116 dBm, communication between nodes can still be achieved. Through point-to-point transmission test, this article finds that in the harsh radio channel environment, compared with the SNR of LoRa, the RSSI of LoRa often has better communication performance, which could ensure the stable communication of nodes. Therefore, the ATP mechanism proposed in this article uses the average SNR of the overall link minus the MAD as the judgment basis. Although this mechanism cannot meet the communication requirements of all nodes in terms of SNR value, the overall connectivity of the link could still be guaranteed by RSSI value and adjusting the TP.

FIGURE 9. Schematic diagram of test environment.

2) SELF-ORGANIZING NETWORK TEST

In order to evaluate the self-organizing network capability of the system and test its fault tolerance, the whole system is experimentally tested. In the test, the power supply voltage was selected as the sensor transmission data. As shown in Fig. 9, the Chemical Road near Northeast Agricultural University was selected as the test site. The distance between two adjacent nodes was about 1 km, and the total length was about 4.9 km. Five nodes were selected for testing, where points A, B, C, and D were sensor node, and point E was a sink node (gateway node). In order to test the fault tolerance of the

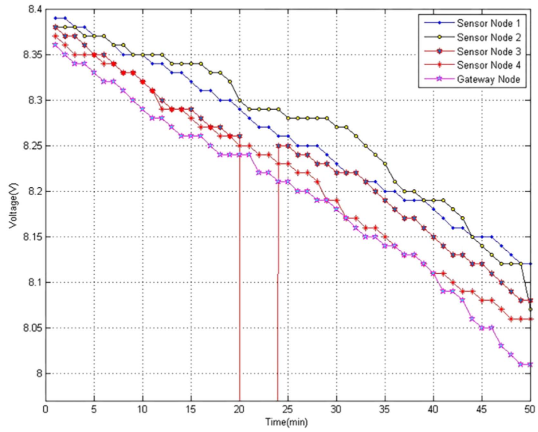

FIGURE 10. Variation curve of node power supply voltage with time.

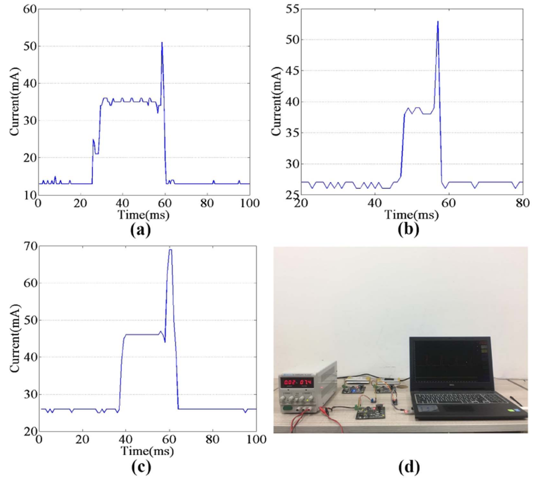

FIGURE 11. Test results and physical photos.

system, the power supply voltage of the third sensor node was cut off at the 20th minute and switched ON again at the 24th minute. The test results are shown in Fig. 10.

During the time when node 3 was disconnected, other nodes transmitted normally. Node 2 became a sink node (gateway node) and formed a linear network with node 1. Node 3, node 4, and sink node (gateway node) formed a new linear network. Fig. 10 shows the power supply voltage variation curve of system nodes, and all voltage values show a downward trend. According to the measured data, the voltage difference between the starting voltage and the ending voltage of the five nodes could be calculated as 0.27 V, 0.31 V, 0.32 V, 0.31 V, and 0.35 V, respectively. During the system operation, the first sensor node consumes the least energy, while the remaining sensor nodes consume similar energy, and gateway node consumes the most energy. In the 20th minute, it could be seen that the power supply voltage of sensor node 3 suddenly changes to 0 V, and the voltage value returns to the normal state in the 24th minute. The total test time was 1 h and 30 min, and data were uploaded once every minute. The cloud received 128 pieces of data. During the test, 130 pieces of data were transmitted, 2 pieces of data were lost, and the overall packet loss rate of the system was 1.538%. In addition, the system could automatically determine that sensor node has failed.

3) WORKING CURRENT TEST

Working current is an important parameter to evaluate the low power consumption performance of the system. In order to evaluate the low power consumption of the system, the working currents of the first sensor node, the last sensor node, and gateway node were measured by INA219 current sensor, respectively. The test results and physical photos are shown in Fig. 11. The time-dependent current curves of the first sensor node, the last sensor node, and sink node are (a), (b), and (c), respectively, and the experimental test diagram is (d). As can be seen from Fig. 11, the lowest current ranges of the three nodes are 10–15 mA, 20–30 mA, and 25–28 mA, respectively, and the peak currents are 60 mA, 53 mA, and 70 mA, respectively. The high current duration of the three nodes is also different. The first and third duration are approximately the same, and the second duration is the shortest. During this period, the current ranges are 50–60 mA, 50–55 mA, and 65–70 mA, respectively.

The low power consumption current of the first sensor node is between 10–20 mA, which is lower than that of the other two nodes. The main reason is that the main control chip STM32F103ZET6 is normally in standby mode instead of sleep mode, and its standby current is only 2 μA, which is much lower than that of subsequent nodes using sleep mode. On the other hand, the peak current of gateway node reached 70 mA, mainly due to the addition of NB-IoT module, thus increasing the energy consumption. The above-mentioned reasons cause the differences in working current. The total current in the low power consumption stage is lower than 30 mA, and the current in the information transmission stage is always between 35 and 60 mA. Although there is some consumption, the lithium battery combined with the solar panel can maintain the long-term stable operation of the system.

4) COMPREHENSIVE TESTING

In order to evaluate the stability of the system for long-term operation, the whole system was tested. In the test, the air temperature was selected as the sensor transmission data. As shown in Fig. 12, the Changjiang Road near The Ash River Nation Wetland Park was selected as the test site. The distance between two adjacent nodes was about 1 km, and the total length was about 3.95 km. The total test time was about 27 h and 40 min. Five nodes were selected for testing, where points A–D were sensor node, and point E was gateway node. The test results are shown in Figs. 13 and 14.

Fig. 13 shows the air temperature variation curve measured by each sensor node. According to the measured data, the temperature dropped rapidly from the initial 15° to below zero, then stabilized and changed with the ambient temperature. The total test time was about 27 h, and data were

FIGURE 12. Schematic diagram of integrated test environment.

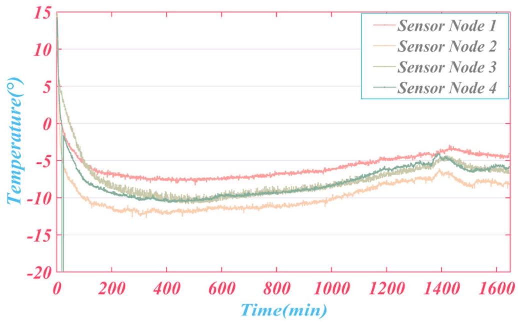

FIGURE 13. Variation curve of air temperature with time.

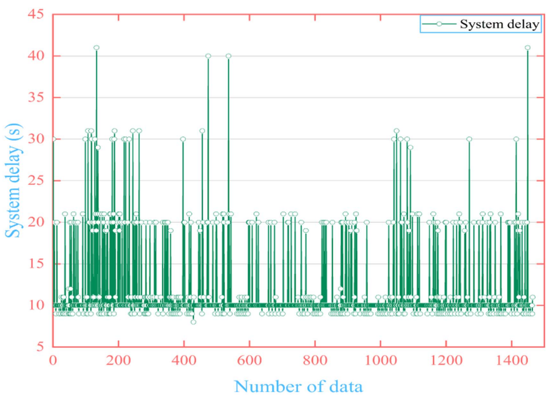

FIGURE 14. System transmission delay.

uploaded once every minute. The cloud received 1464 pieces of data. During the test, 1467 pieces of data were transmitted, 3 pieces of data were lost, and the overall packet loss rate of the system was 0.1829%. Fig. 14 shows the transmission delay of 1464 pieces of data in the system. The delay calculation of each piece of data is that the first node starts to transmit data and ends when the sink node receives the aggregated data. According to the measurement data, most of the delays are in the interval of 10–20 s. A few delays exceed 20 s, which is caused by multiple data retransmissions of the system.

V. CONCLUSION

The main contribution of this study is to propose an energy-saving LoRa linear network with ATP. In this network, new LPWAN technologies are adopted, including LoRa communication and NB-IoT communication. In particular, the system adopts ATP mechanism, flexible self-organizing network, and optimized duty cycling policy, which could reduce energy consumption while improving communication quality. Through the point-to-point transmission test, the experimental data support is provided for the theoretical establishment of the ATP mechanism in this article. The simulation experiments and field test results show that the system runs stably and can locate fault nodes quickly, with strong robustness, reliability, scalability, and fault tolerance. At present, this study is one of the few linear networks that could accurately adjust the transmission parameters of LoRa multihop, which has instructive significance for the application of LoRa in WSNs.

REFERENCES

[1] A. Al-Fuqaha, M. Guizani, M. Mohammadi, M. Aledhari, and M. Ayyash, "Internet of Things: A survey on enabling technologies, protocols, and applications," *IEEE Commun. Surveys Tuts.*, vol. 17, no. 4, pp. 2347–2376, Oct.–Dec. 2015.

[2] S. Chen, H. Xu, D. Liu, B. Hu, and H. Wang, "A vision of IoT: Applications, challenges, and opportunities with China perspective," *IEEE Internet Things J.*, vol. 1, no. 4, pp. 349–359, Aug. 2014.

[3] A. Zanella, N. Bui, A. Castellani, L. Vangelista, and M. Zorzi, "Internet of Things for smart cities," *IEEE Internet Things J.*, vol. 1, no. 1, pp. 22–32, Feb. 2014.

[4] L. Catarinucci et al., "An IoT-aware architecture for smart healthcare systems," *IEEE Internet Things J.*, vol. 2, no. 6, pp. 515–526, Dec. 2015.

[5] I. Jawhar et al., "Linear wireless sensor networks: Classification and applications," *J. Netw. Comput. Appl.*, vol. 34, no. 5, pp. 1671–1682, Sep. 2011.

[6] U. Raza, P. Kulkarni, and M. Sooriyabandara, "Low power wide area networks: An overview," *IEEE Commun. Surveys Tuts.*, vol. 19, no. 2, pp. 855–873, Apr.–Jun. 2017.

[7] A. J. Wixted, P. Kinnaird, H. Larijani, A. Tait, A. Ahmadinia, and N. Strachan, "Evaluation of LoRa and LoRaWAN for wireless sensor networks," in *Proc. IEEE Sensors*, 2016, pp. 1–3.

[8] R. El Chall, S. Lahoud, and M. El Helou, "LoRaWAN network: Radio propagation models and performance evaluation in various environments in Lebanon," *IEEE Internet Things J.*, vol. 6, no. 2, pp. 2366–2378, Apr. 2019.

[9] M. I. Muzammir, H. Z. Abidin, S. A. C. Abdullah, and F. H. K. Zaman, "Performance analysis of LoRaWAN for indoor application," in *Proc. IEEE 9th Symp. Comput. Appl. Ind. Electron.*, 2019, pp. 156–159.

[10] D. Davcev, K. Mitreski, S. Trajkovic, V. Nikolovski, and N. Koteli, "IoT agriculture system based on LoRaWAN," in *Proc. IEEE 14th Int. Workshop Factory Commun. Syst.*, 2018, pp. 1–4.

[11] G. Yang and H. Liang, "A smart wireless paging sensor network for elderly care application using LoRaWAN," *IEEE Sensors J.*, vol. 18, no. 22, pp. 9441–9448, Nov. 2018.

[12] X. Xiong, K. Zheng, R. Xu, W. Xiang, and P. Chatzimisios, "Low power wide area machine-to-machine networks: Key techniques and prototype," *IEEE Commun. Mag.*, vol. 53, no. 9, pp. 64–71, Sep. 2015.

[13] T. Elshabrawy and J. Robert, "Capacity planning of LoRa networks with joint noise-limited and interference-limited coverage considerations," *IEEE Sensors J.*, vol. 19, no. 11, pp. 4340–4348, Jun. 2019.

[14] F. Adelantado, X. Vilajosana, P. Tuset-Peiro, B. Martinez, J. Melia-Segui, and T. Watteyne, "Understanding the limits of LoRaWAN," *IEEE Commun. Mag.*, vol. 55, no. 9, pp. 34–40, Sep. 2017.

[15] M. H. Dwijaksara, W. Sook Jeon, and D. G. Jeong, "Multihop gateway-to-gateway communication protocol for LoRa networks," in *Proc. IEEE Int. Conf. Ind. Technol.*, 2019, pp. 949–954.

[16] M. O. Farooq, "Multi-hop communication protocol for LoRa with software-defined networking extension," *Internet Things*, vol. 14, 2021, Art. no. 100379.
[17] A. Abrardo, A. Fort, E. Landi, M. Mugnaini, E. Panzardi, and A. Pozzebon, "Black powder flow monitoring in pipelines by means of multi-hop LoRa networks," in *Proc. II Workshop Metrol. Ind. 4.0 IoT*, 2019, pp. 312–316.
[18] A. Abrardo and A. Pozzebon, "A multi-hop LoRa linear sensor network for the monitoring of underground environments: The case of the medieval aqueducts in Siena," *Sensors*, vol. 19, no. 2, pp. 402–423, 2019.
[19] C. Ebi, F. Schaltegger, A. Rüst, and F. Blumensaat, "Synchronous LoRa mesh network to monitor processes in underground infrastructure," *IEEE Access*, vol. 7, pp. 57663–57677, 2019.
[20] C. Cano, B. Bellalta, A. Sfairopoulou, and J. Barcelo, "A low power listening MAC with scheduled wake up after transmissions for WSNs," *IEEE Commun. Lett.*, vol. 13, no. 4, pp. 221–223, Apr. 2009.
[21] Z. Rezaei and S. Mobininejad, "Energy saving in wireless sensor networks," *Int. J. Comput. Sci. Eng. Surv.*, vol. 3, no. 1, pp. 23–37, Feb. 2012.
[22] V. P. Nighot, S. M. Lambor, and S. M. Joshi, "Efficient battery management in wireless sensor node: Review paper," in *Proc. 11th Int. Conf. Wireless Opt. Commun. Netw.*, 2014, pp. 1–5.
[23] X. Zhang, M. Zhang, F. Meng, Y. Qiao, S. Xu, and S. Hour, "A low-power wide-area network information monitoring system by combining NB-IoT and LoRa," *IEEE Internet Things J.*, vol. 6, no. 1, pp. 590–598, Feb. 2019.
[24] X. Zhang, J. Du, C. Fan, D. Liu, J. Fang, and L. Wang, "A wireless sensor monitoring node based on automatic tracking solar-powered panel for paddy field environment," *IEEE Internet Things J.*, vol. 4, no. 5, pp. 1304–1311, Oct. 2017.
[25] M. C. Bor, U. Roedig, T. Voigt, and J. M. Alonso, "Do LoRa low-power wide-area networks scale?," in *Proc. 19th ACM Int. Conf. Model., Anal., Simul. Wireless Mobile Syst.*, 2016, pp. 59–67.
[26] H.-C. Lee and K.-H. Ke, "Monitoring of large-area IoT sensors using a LoRa wireless mesh network system: Design and evaluation," *IEEE Trans. Instrum. Meas.*, vol. 67, no. 9, pp. 2177–2187, Sep. 2018.
[27] D. L. Mai and M. K. Kim, "Multi-hop LoRa network with pipelined transmission capability," in *Proc. Ubiquitous Netw.: 5th Int. Symp.*, 2020, pp. 125–135.

HAO WANG received the B.E. degree in electrical engineering and automation in 2021 from Northeast Agricultural University, Harbin, China, where he is currently working toward the M.D. degree in computer science and technology.

His current research interest is intelligent control technology.

SHANSHAN LV received the B.E. degree in software engineering from Harbin University of Science and Technology, Harbin, China, in 2021. He is currently working toward the M.D. degree in computer science and technology with Northeast Agricultural University, Harbin.

His current research interest includes the Internet of Things technology.

YANG HAN received the B.E. degree in automation from Shandong University of Technology, Zibo, China, in 2022. He is currently working toward the M.D. degree in electrical engineering with Northeast Agricultural University, Harbin, China.

His current research interest includes the sensing technology.

XIHAI ZHANG (Member, IEEE) was born in Harbin, China, in 1979. He received the B.S. and M.S. degrees in electrical engineering from Northeast Agricultural University, Harbin, China, in 2002 and 2005, respectively, and the Ph.D. degree in control science and engineering from Harbin Institute Technology, Harbin, in 2013.

He is currently a Professor with the College of Electronics and Information, Northeast Agricultural University. His current research interests include the Internet of Things, embedded systems, as well as deep learning and its application to computer vision and pattern recognition.

YU ZHANG was born in Harbin, China, in 1984. He received the B.S. and Ph.D. degrees in underwater acoustic engineering from Harbin Engineering University, Harbin, China, in 2007 and 2014, respectively.

He is currently a Lecturer with the College of Electronics and Information, Northeast Agricultural University, Harbin. His current research interests include the Internet of Things, applications to embedded systems, as well as software development.

WENBIN DONG received the B.E. degree in electronic information science and technology from Hebei Agricultural University, Baoding, China, in 2018. He is currently working toward the M.D. degree in computer science and technology with Northeast Agricultural University, Harbin, China.

His current research interest is intelligent control technology.

JIANXIN LIAO received the B.E. degree in electronic information science and technology from Shandong University of Science and Technology, Taian, China, in 2020, and the M.D. degree in computer science and technology from Northeast Agricultural University, Harbin, China, in 2023.

He is currently with State Grid Zoucheng Power Supply Company, Zoucheng, China. His research interest is the Internet of Things.

HONGWEI LUAN received the B.E. degree in network engineering from Harbin University of Science and Technology, Harbin, China, in 2008. He is currently working toward the M.D. degree in agricultural engineering and information technology with Northeast Agricultural University, Harbin.

His current research interest is wireless network communication.